Polyhedral Metallacarbaborane Chemistry: Preparation, Molecular Structure, and Nuclear Magnetic Resonance Investigation of [3-(η^5-C_5Me_5)-*closo*-3,1,2-$MC_2B_9H_{11}$] (M = Rh or Ir)†

Xavier L. R. Fontaine, Norman N. Greenwood, John D. Kennedy, Karl Nestor, and Mark Thornton-Pett
School of Chemistry, University of Leeds, Leeds LS2 9JT
Stanislav Heřmánek, Tomáš Jelínek, and Bohumil Štíbr
Institute of Inorganic Chemistry, Czechoslovak Academy of Sciences, 25068 Řež u Prahy, Czechoslovakia

Reaction between Cs[*nido*-7,8-$C_2B_9H_{11}$] and [{M(η^5-C_5Me_5)Cl_2}$_2$] (M = Rh or Ir) yielded orange-yellow, air-stable crystals of [3-(η^5-C_5Me_5)-*closo*-3,1,2-$RhC_2B_9H_{11}$] [compound (**2**), 34%] or [3-(η^5-C_5Me_5)-*closo*-3,1,2-$IrC_2B_9H_{11}$] [compound (**3**), 96%] both of which were characterized by their assigned ^{11}B and ^{1}H n.m.r. spectra and by single-crystal *X*-ray diffraction analyses. Crystals of (**2**) were orthorhombic, space group $P2_12_12_1$, with a = 1 081.0(2), b = 1 278.2(1), c = 1 278.4(2) pm, and Z = 4; R = 0.0197, R' = 0.0204 for 1 756 observed reflections [$I > 2.0\sigma(I)$]. Crystals of (**3**) were also orthorhombic, space group $P2_12_12_1$, with a = 1 076.3(1), b = 1 282.9(1), c = 1 292.8(2) pm, and Z = 4; R = 0.0286, R' = 0.0307, for 1 712 observed reflections [$I > 2.0\sigma(I)$]. The n.m.r. properties of the $C_2B_9H_{11}$ fragments of (**2**) and (**3**) are compared with the ^{11}B and hitherto unreported ^{1}H n.m.r. characteristics of the corresponding fragments of [3-(η^5-C_5H_5)-*closo*-3,1,2-$CoC_2B_9H_{11}$] (**4**), *closo*-1,2-$C_2B_{10}H_{12}$, *nido*-7,8-$C_2B_9H_{13}$, and [*nido*-7,8-$C_2B_9H_{12}$]$^-$, in order to assess any n.m.r. shielding patterns that might reveal bonding trends. The unique *endo*/bridging open-face hydrogen atom in [*nido*-7,8-$C_2B_9H_{12}$]$^-$ is discussed in the light of its n.m.r. properties.

We have previously reported preparative, structural, and n.m.r. details of the twelve-vertex *closo*-3,1,2-metalladicarbaborane [(η^6-C_6Me_6)$RuC_2B_9H_{11}$] (**1**).[1,2] Here we report corresponding investigations of the previously unreported rhodium and iridium analogues [3-(η^5-C_5Me_5)-*closo*-3,1,2-$RhC_2B_9H_{11}$] (**2**) and [3-(η^5-C_5Me_5)-*closo*-3,1,2-$IrC_2B_9H_{11}$] (**3**), together with n.m.r. studies of the known[3,4] cobalt species [3-(η^5-C_5H_5)-*closo*-3,1,2-$CoC_2B_9H_{11}$] (**4**) for comparison. N.m.r. studies on the two non-metallated eleven-vertex *nido*-dicarbaborane species *nido*-7,8-$C_2B_9H_{13}$ and [*nido*-7,8-$C_2B_9H_{12}$]$^-$ have also been carried out in order to assess the extent and nature of perturbation of the *nido*-7,8-$C_2B_9H_{11}$ fragment upon complexation to the Rh(η^5-C_5Me_5) and Ir(η^5-C_5Me_5) moieties. Related work on the incorporation of fragments such as M(η^n-C_nMe_n) (M = second- or third-row transition element, n = 5 or 6) to form metallaborane or metallaheteroborane cluster compounds has been reported recently for rhodium,[5–10] iridium,[9–13] and ruthenium.[1,2,5,8,9,14,15] The *nido* eleven-vertex and *closo* twelve-vertex numbering systems used in this work are as in structures (**I**) and (**II**) respectively.

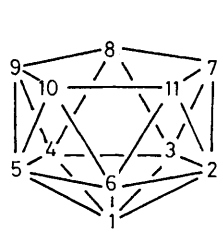

(I)

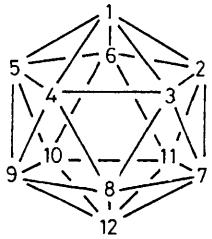

(II)

Results and Discussion

The reaction between [{M(η^5-C_5Me_5)Cl_2}$_2$] (M = Rh or Ir) and the *nido*-anion [7,8-$C_2B_9H_{12}$]$^-$ in dichloromethane solution in the presence of *N,N,N',N'*-tetramethylnaphthalene-1,8-diamine (tmnd) as base, followed by chromatographic separation and purification, readily yielded air-stable, orange crystals of [3-(η^5-C_5Me_5)-*closo*-3,1,2-$MC_2B_9H_{11}$], where M = Rh [compound (**2**), 34% yield] or Ir [compound (**3**), 96% yield]. The stoicheiometry of formation is straightforward [equation (1)].

$$\tfrac{1}{2}[\{M(\eta^5\text{-}C_5Me_5)Cl_2\}_2] + Cs[C_2B_9H_{12}] + tmnd \longrightarrow [(\eta^5\text{-}C_5Me_5)MC_2B_9H_{11}] + [Htmnd]Cl + CsCl \quad (1)$$

Both compounds readily recrystallized from dichloromethane–hexane solutions to give crystals suitable for single-crystal *X*-ray diffraction analyses. Derived interatomic distances and angles are in Tables 1 and 2 and drawings of the molecular structures are in Figure 1. The compounds were found to be isomorphous, with measured unit-cell dimensions and volumes differing by $\leqslant$ *ca.* 1%, and the final solutions differed only marginally in the methyl-group rotamers of the C_5Me_5 groups. Within experimental error the molecular structures for the two compounds were found to be identical, as can be seen from the comparisons within horizontal rows in Tables 1 and 2.

From Figure 1 it is clear that each compound is a *closo* twelve-vertex species with the metal and the two adjacent carbon atoms forming one triangular face of the icosahedron. The dimensions within the MC_2B_9 clusters are very similar indeed to those previously reported[2] for the arene ruthenium analogue [3-(η^6-C_6Me_6)-*closo*-3,1,2-$RuC_2B_9H_{11}$] (**1**), the principal differences being that in (**2**) and (**3**) the metal appears to be held marginally more compactly in the cluster (by *ca.* 3 pm), and that the hint of

† 3-η-Pentamethylcyclopentadienyl-1,2-dicarba-3-rhoda(or-irida)-*closo*-dodecaborane.

Supplementary data available: see Instructions for Authors, *J. Chem. Soc., Dalton Trans.*, 1990, Issue 1, pp. xix—xxii.

Table 1. Interatomic distances (in pm) for [3-(η^5-C_5Me_5)-*closo*-3,1,2-$MC_2B_9H_{11}$], where M = Rh [compound (**2**), first two columns] or Ir [compound (**3**), second two columns], with estimated standard deviations (e.s.d.s) in parentheses*

From the metal atom							
Rh(3)–C(1)	216.9(5)	Rh(3)–C(2)	217.2(5)	Ir(3)–C(1)	217.4(12)	Ir(3)–C(2)	215.8(11)
Rh(3)–B(4)	218.5(6)	Rh(3)–B(7)	218.7(6)	Ir(3)–B(4)	214.1(13)	Ir(3)–B(7)	218.0(12)
Rh(3)–B(8)	217.3(6)	—	—	Ir(3)–B(8)	220.8(14)	—	—
Rh(3)–C(11)	216.9(5)	Rh(3)–C(15)	215.1(5)	Ir(3)–C(11)	215.7(11)	Ir(3)–C(15)	216.2(11)
Rh(3)–C(12)	220.9(5)	Rh(3)–C(14)	217.9(5)	Ir(3)–C(12)	222.4(11)	Ir(3)–C(14)	219.6(11)
Rh(3)–C(13)	223.0(5)	—	—	Ir(3)–C(13)	222.6(11)	—	—
Boron–carbon							
C(1)–B(4)	173.7(8)	C(2)–B(7)	171.0(8)	C(1)–B(4)	172.4(18)	C(2)–B(7)	176.5(17)
C(1)–B(5)	169.6(7)	C(2)–B(11)	169.9(7)	C(1)–B(5)	167.4(16)	C(2)–B(11)	168.4(16)
C(1)–B(6)	172.5(7)	C(2)–B(6)	172.7(7)	C(1)–B(6)	169.1(16)	C(2)–B(6)	171.5(17)
Boron–boron							
B(4)–B(5)	179.2(8)	B(7)–B(11)	178.2(8)	B(4)–B(5)	180.3(17)	B(7)–B(11)	179.8(17)
B(4)–B(8)	180.0(8)	B(7)–B(8)	181.8(9)	B(4)–B(8)	187.9(18)	B(7)–B(8)	177.9(18)
B(4)–B(9)	175.0(8)	B(7)–B(12)	176.1(8)	B(4)–B(9)	180.9(18)	B(7)–B(12)	175.6(18)
B(5)–B(6)	176.0(8)	B(11)–B(6)	175.2(9)	B(5)–B(6)	169.5(19)	B(11)–B(6)	181.5(19)
B(5)–B(10)	174.9(9)	B(11)–B(10)	176.3(9)	B(5)–B(10)	165.9(19)	B(11)–B(10)	174.6(18)
B(5)–B(9)	176.6(9)	B(11)–B(12)	176.6(10)	B(5)–B(9)	173.9(20)	B(11)–B(12)	169.4(21)
B(8)–B(9)	177.7(8)	B(8)–B(12)	178.1(8)	B(8)–B(9)	178.6(18)	B(8)–B(12)	174.6(18)
B(9)–B(10)	178.4(9)	B(12)–B(10)	177.7(8)	B(9)–B(10)	176.4(19)	B(12)–B(10)	176.6(19)
B(9)–B(12)	177.2(9)	—	—	B(9)–B(12)	173.2(20)	—	—
Carbon–carbon							
C(1)–C(2)	163.5(7)	—	—	C(1)–C(2)	162.4(14)	—	—
C(11)–C(12)	142.8(6)	C(15)–C(14)	142.0(6)	C(11)–C(12)	146.2(16)	C(15)–C(14)	139.6(15)
C(11)–C(15)	143.8(6)	—	—	C(11)–C(15)	146.0(15)	—	—
C(11)–C(16)	148.6(6)	C(15)–C(110)	150.8(7)	C(11)–C(16)	148.9(14)	C(15)–C(110)	151.5(16)
C(12)–C(13)	144.2(6)	C(14)–C(13)	141.8(6)	C(12)–C(13)	138.8(14)	C(14)–C(13)	140.5(15)
C(12)–C(17)	148.8(6)	C(14)–C(19)	151.8(7)	C(12)–C(17)	147.4(15)	C(14)–C(19)	150.0(16)
C(13)–C(18)	150.3(7)	—	—	C(13)–C(18)	151.4(16)	—	—
Boron–hydrogen and carbon–hydrogen							
C(1)–H(1)	105.6	C(2)–H(2)	108.7	C(1)–H(1)	107.7	C(2)–H(2)	111.4
B(4)–H(4)	104.2	B(7)–H(7)	125.1	B(4)–H(4)	106.9	B(7)–H(7)	119.9
B(5)–H(5)	115.0	B(11)–H(11)	117.7	B(5)–H(5)	123.5	B(11)–H(11)	117.6
B(6)–H(6)	96.6	—	—	B(6)–H(6)	100.6	—	—
B(8)–H(8)	110.0	—	—	B(8)–H(8)	108.1	—	—
B(9)–H(9)	119.1	B(12)–H(12)	91.5	B(9)–H(9)	121.8	B(12)–H(12)	93.1
B(10)–H(10)	113.8	—	—	B(10)–H(10)	115.8	—	—

* Horizontal rows contain distances that would be identical if both molecules were identical and had the mirror-plane symmetry to which they approximate.

slippage from *closo* to *nido* geometry (as manifested more strongly, for example, in certain platinadicarbaboranes[16,17]) appears to be marginally greater for the rhodium and iridium species (**2**) and (**3**) than for the ruthenium compound (**1**); thus the angles of tilt between the η^5-C_5 and η^5-C_2B_3 planes are 8.1 and 7.6° for (**2**) and (**3**) respectively compared with *ca.* 3° for (**1**). This minimal slippage contrasts to the situation with corresponding eleven-vertex ruthenium and iridium metalladicarbaundecaborane species such as [1-(η^6-MeC_6H_4-Pr^i-4)-*closo*-1,2,4-$RuC_2B_8H_8$][15,18] and [1,1,1-$(PPh_3)_2$H-*closo*-1,2,4-$IrC_2B_8H_{10}$][19] which exhibit considerable distortion from closed to give *isonido*-type geometries that are more open.[10,15,18,19]

Compounds (**2**) and (**3**) can therefore be considered essentially as straightforward Williams–Wade[20,21] *closo* cluster species, with the M(η^5-C_5Me_5) moieties supplying three orbitals and two electrons to the cluster bonding scheme, just like BH. In metal-complex terms the compounds are 'octahedral' complexes of rhodium(III) and iridium(III); in metal–ligand terms they are complexes between M(η^5-C_5Me_5)$^{2+}$ and *pentahapto*-$[C_2B_9H_{11}]^{2-}$, and in cluster terms they are analogues of $C_2B_{10}H_{12}$ or $[B_{12}H_{12}]^{2-}$. These considerations can be explored somewhat by comparison of the n.m.r. properties of compounds (**1**)—(**3**), and of *closo*-1,2-$C_2B_{10}H_{12}$, *nido*-7,8-$C_2B_9H_{13}$, and [*nido*-$C_2B_9H_{12}$]$^-$ as discussed below.

The measured n.m.r. properties of [3-(η^5-C_5Me_5)-*closo*-3,1,2-$MC_2B_9H_{11}$] [M = Rh (**2**) and Ir (**3**)] are in Table 3. Also included for comparison are data for the cobalt analogue [3-(η^5-C_5H_5)-*closo*-3,1,2-$CoC_2B_9H_{11}$] (**4**). Although this last compound has been known for some time,[3,4] comprehensive and assigned cluster ^{11}B and ^{1}H n.m.r. data have not previously been reported. The present assignments were made by {^{11}B-^{11}B}-COSY, ^{1}H-{^{11}B(selective)}, and [^{1}H-^{1}H]-COSY-{^{11}B} experiments. The observed [^{11}B-^{11}B] correlations were largely similar to those mentioned elsewhere[1] for the ruthenium analogue [3-(η^6-C_6Me_6)-*closo*-3,1,2-$RuC_2B_9H_{11}$] (**1**), again noteworthy being the weaker [^{11}B-^{11}B]-COSY interactions for the B(6) position that is connected to both skeletal carbon positions, a phenomenon that is of general character for interboron linkages flanking heteroatoms. A second interesting correlation is the ^4J(^{1}H–C–B–B–^{1}H) one between ^{1}H(1,2) and ^{1}H(8), all other interproton correlations being *via* straightforward ^3J pathways.

Some of the results are presented graphically in Figure 2, in which the upper diagram is a plot of δ(^{1}H) *versus* δ(^{11}B) for the

Table 2. Selected angles (°) between interatomic vectors for compounds (**2**) and (**3**) with e.s.d.s in parentheses

	Compound (**2**)	Compound (**3**)		Compound (**2**)	Compound (**3**)
About the metal atom					
C(1)–M(3)–C(2)	44.3(1)	44.0(3)			
C(1)–M(3)–B(4)	47.0(1)	47.1(4)	C(2)–M(3)–B(7)	46.2(2)	48.0(4)
C(1)–M(3)–B(7)	78.9(2)	81.2(5)	C(2)–M(3)–B(4)	79.6(2)	79.5(5)
C(1)–M(3)–B(8)	80.3(2)	81.7(5)	C(2)–M(3)–B(8)	80.3(3)	79.9(5)
B(4)–M(3)–B(8)	48.8(2)	51.2(5)	B(7)–M(3)–B(8)	49.3(2)	47.8(4)
B(4)–M(3)–B(7)	83.3(3)	85.1(5)			
About the cluster carbon atoms					
M(3)–C(1)–C(2)	68.0(3)	67.4(6)	M(3)–C(2)–C(1)	67.8(3)	68.5(6)
M(3)–C(1)–B(4)	67.0(3)	65.5(6)	M(3)–C(2)–B(7)	67.4(3)	66.6(6)
M(3)–C(1)–B(5)	124.7(4)	122.9(8)	M(3)–C(2)–B(11)	125.0(4)	124.2(8)
M(3)–C(1)–B(6)	125.9(3)	126.1(7)	M(3)–C(2)–B(6)	125.6(3)	125.8(7)
B(4)–C(1)–C(2)	111.6(4)	110.3(9)	B(7)–C(2)–C(1)	111.7(4)	113.3(9)
B(5)–C(1)–C(2)	110.9(4)	107.9(9)	B(11)–C(2)–C(1)	110.6(4)	112.2(9)
B(6)–C(1)–C(2)	61.8(3)	62.3(7)	B(6)–C(2)–C(1)	61.7(3)	60.8(7)
B(4)–C(1)–B(5)	62.9(3)	64.1(8)	B(7)–C(2)–B(11)	63.0(4)	62.8(7)
B(4)–C(1)–B(6)	114.5(4)	115.8(9)	B(7)–C(2)–B(6)	114.4(4)	117.3(9)
B(5)–C(1)–B(6)	61.9(3)	60.5(8)	B(11)–C(2)–B(6)	61.5(4)	64.5(8)
Others					
B–B–Ir(acute)	65.0(3)—66.0(3)	62.6(6)—66.9(6)	B–B–C(obtuse)	103.5(4)—105.5(4)	99.1(9)—107.9(9)
B–B–Ir(obtuse)	118.3(4)—119.8(4)	115.5(8)—118.2(8)	B–B–B(acute)	58.6(3)—61.3(3)	56.5(8)—63.3(8)
B–B–C(acute)	57.4(3)—59.9(3)	56.4(7)—60.8(7)	B–B–B(obtuse)	106.2(4)—110.2(4)	104.0(8)—112.5(9)
Dihedral angles					
B(4)B(7)B(8)–η^5-C_5Me_5	7.1(3)	3.6(8)	B(4)B(7)B(8)–B(4)C(1)C(2)B(7)	1.6(3)	6.2(8)

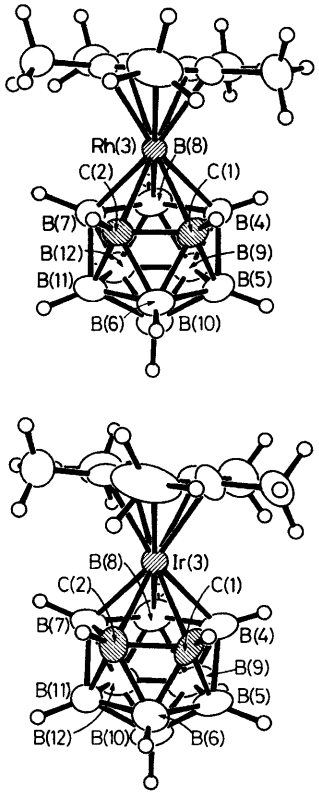

Figure 1. ORTEP drawings of the crystallographically determined molecular structures of [3-(η^5-C_5Me_5)-*closo*-3,1,2-$RhC_2B_9H_{11}$] (**2**) (top) and of [3-(η^5-C_5Me_5)-*closo*-3,1,2-$IrC_2B_9H_{11}$] (**3**) (bottom)

BH units in the ruthenium, rhodium, iridium, and cobalt compounds (**1**), (**2**), (**3**), and (**4**) respectively. In contrast to many polyhedral boron-containing compounds (see, for example, *nido*-7,8-$C_2B_9H_{13}$ and [*nido*-7,8-$C_2B_9H_{12}$]$^-$, Figure 3) there are considerable deviations from a reasonably linear $\delta(^1H)$ *vs.* $\delta(^{11}B)$ correlation. Thus, compared to a correlation line similar to those found useful for the assessment of (^{11}B, ^1H) shielding patterns in other twelve-vertex *closo*-metallaheteroboranes,[8,22–25] the BH(8) and BH(4,7) units of compounds (**1**)—(**4**) exhibit somewhat enhanced ^1H shielding. This also occurs for the twelve-vertex metallatelluraboranes [2-(η^n-C_nMe_n)-*closo*-2,1-$MTeB_{10}H_{10}$] (M = Ru, n = 6; or M = Rh, n = 5) and has been tentatively accounted for[8] in terms of possible C_nMe_n non-bonded interaction with these cluster α-hydrogen atoms. However, the similar ^1H(4, 7) and ^1H(8) shielding behaviour now observed for the (η^5-C_5H_5) cobalt compound (**4**) would perhaps tend not to support this particular hypothesis. A more dramatic deviation is afforded by the BH(10) unit for the iridium species (**3**) which exhibits a $\delta(^1H)$ value some 2 p.p.m. to low field of the first-row and second-row transition-metal analogues (**1**), (**2**), and (**4**). This antipodal heavy-atom effect on proton shielding [structure (**III**)] has been noted in other *closo* twelve-vertex systems[8,22–25] and now seems reasonably diagnostic of an antipodal heavy

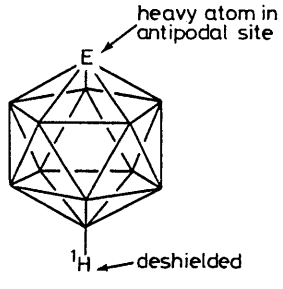

(**III**)

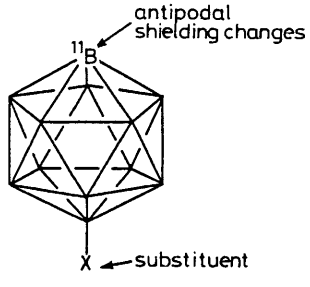

(**IV**)

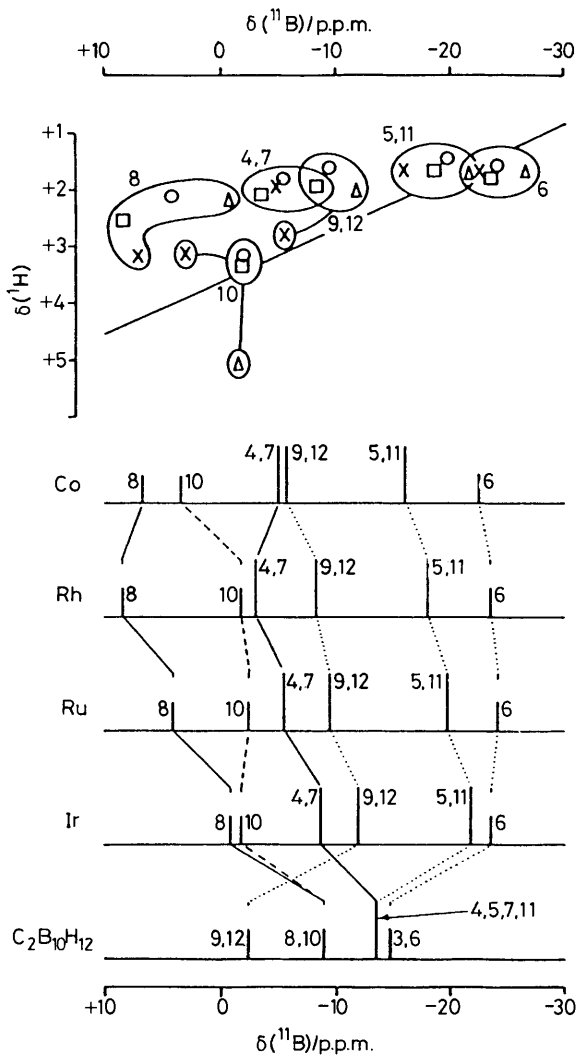

Figure 2. The upper diagram is a plot of $\delta(^1H)$ *versus* (^{11}B) for directly bound ^1H and ^{11}B in the rhodium compound (**2**) (□), the iridium compound (**3**) (△) the 3-(η^6-C_6Me_6)-3-Ru analogue (**1**) (○) (data from ref 2), and the cobalt compound (**4**) (×). The line drawn has slope $\delta(^1H)$ *vs.* $\delta(^{11}B)$ of *ca.* 1:11, with intercept +3.6 p.p.m. in $\delta(^1H)$. These coefficients are similar to those for correlation lines found useful in the assessment of similar plots for other closed twelve-vertex metallaheteroboranes (refs. 8 and 22—25). The lower diagram [same scale in $\delta(^{11}B)$] shows stick representations of the chemical shifts and relative intensities in the ^{11}B n.m.r. spectra of (**1**), (**2**), and (**3**), together with those of [3-(η^5-C_5H_5)-*closo*-3,1,2-$CoC_2B_9H_{11}$] (**4**) and *closo*-1,2-$C_2B_{10}H_{12}$ for comparison. Lines join equivalent positions in the five species: (——) adjacent (α) to metal centre (• • • •) β to metal centre, and (– – – –) antipodal (γ) to metal centre

atom position. It is in some respects complementary to the *exo* substituent effects[26] on the shielding of the *cluster* nuclei in antipodal positions [structure (**IV**)]. Another ostensible deviation from the $\delta(^1H)$ *vs.* $\delta(^{11}B)$ general trend is the behaviour of the BH(10) and BH(9, 12) positions, antipodal to the Co(3) and CH(1, 2) positions respectively in (**4**), which are both somewhat downfield in the ^{11}B n.m.r. spectrum. However, this arises from an ^{11}B shielding change rather than a ^1H anomaly.

The lower diagram in Figure 2 compares the appearance of the ^{11}B n.m.r. chemical shift patterns of compounds (**1**)—(**4**) with those of the non-metal-containing dicarbaborane analogue *closo*-1,2-$C_2B_{10}H_{12}$ (data in Table 4) from which the metalladicarbaboranes are notionally derived by the replacement of the

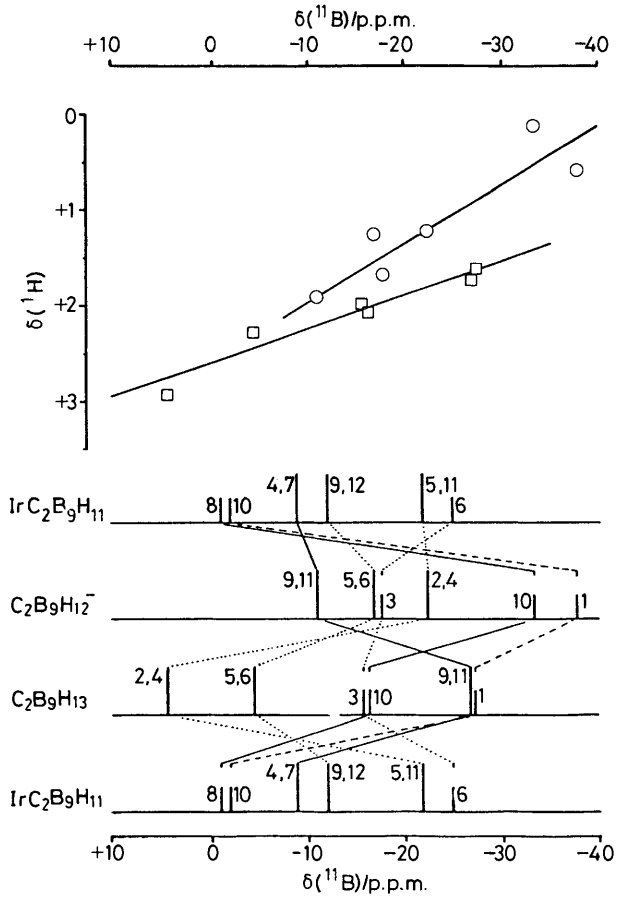

Figure 3. The upper diagram is a plot of $\delta(^1H)$(*exo*)*versus* $\delta(^{11}B)$ for directly attached BH(*exo*) units in neutral 7,8-$C_2B_9H_{13}$ (□) and in the [7,8-$C_2B_9H_{12}$]$^-$ anion (○). The upper line drawn has slope $\delta(^1H)$ *vs.* $\delta(^{11}B)$ 1:16, intercept +2.6 p.p.m. in $\delta(^1H)$, and the lower one slope 1:28 with intercept +2.6 p.p.m. in $\delta(^1H)$. The lower diagram [same scale in $\delta(^{11}B)$] gives (centre two traces) stick representations of the chemical shifts and relative intensities in the ^{11}B n.m.r. spectra of $C_2B_9H_{13}$ and [$C_2B_9H_{12}$]$^-$, together with similar representations (topmost and lowest traces) of [3-(η^5-C_5Me_5)-*closo*-3,1,2-$IrC_2B_9H_{11}$] (**3**) for comparison. Lines join equivalent sites in the three species: (——) adjacent (α) to the metal atom, (• • • •) β to the metal atom, and (– – – –) antipodal (γ) to the metal atom

BH unit in the 3 position by the metal centres.[1,2] It can be seen that the shift patterns for all four metalladicarbaborane compounds are very closely related, emphasizing their similarities in cluster electronic structure. The main variations among the four compounds occur at the 8 position adjacent to the metal centre. The changes at the 10 positions antipodal to the metal atoms are very small indeed among compounds (**1**)—(**3**), although the data for the cobalt compound (**4**) show that the first-row element generates a more significant effect. It can also be seen that there is a close relationship to the *closo*-1,2-$C_2B_{10}H_{12}$ parent model compound: compared to this dicarbaborane, the iridium compound (**3**) (taken as the closest example) shows a *ca.* 10 p.p.m. deshielding at the (4,7) and (8) positions adjacent to the metal centre [a general phenomenon as also found for example in *nido*-5- and -6-metalladecaboranes containing M(η^n-C_nMe_n) units],[8,9,27] together with a metal-antipodal deshielding effect of similar magnitude. Concomitant with these decreases, there is an increase in shielding at the other cluster ^{11}B positions resulting in a conservation of 'cluster chemical shift' [mean chemical shifts of compound (**3**) and 1,2-$C_2B_{10}H_{12}$ are −12.6 and −11.8 p.p.m. respectively]. These similarities support the suggestion that the cluster highest occupied molecular orbitals

Table 3. Measured n.m.r. parameters (δ/p.p.m., *J*/Hz) of [3-(η^5-C_5X_5)-*closo*-3,1,2-$MC_2B_9H_{11}$] where X = Me, M = Rh (**2**), X = Me, M = Ir (**3**), and X = H, M = Co (**4**) in CD_2Cl_2 solution at 294—297 K

Assignment[a]	Compound (**2**) δ(^{11}B)	$^1J(^{11}B-^1H)$	δ(^{1}H)[b]	Compound (**3**) δ(^{11}B)	$^1J(^{11}B-^1H)$	δ(^{1}H)[b]	Observed [^{11}B–^{11}B]-COSY correlations[c,d]	Observed [^{1}H–^{1}H]-COSY correlation[c,e]	Compound (**4**) δ(^{11}B)	$^1J(^{11}B-^1H)$	δ(^{1}H)[b]
1, 2	—	—	+3.29[f]	—	—	+3.61[f]	—	(4, 7)m (5, 11)s 6s 8w[4]	—	—	+4.08[f]
3	—	—	+2.04[g]	—	—	+2.09[g]	—	—	—	—	+5.67[g]
4, 7	−3.5	152	+2.08	−8.7	153	+1.98	(5, 11)m 8s (9, 12)s	(1, 2)m (5, 11)s 8s? (9, 12)s	−4.9	*h*	+1.92
5, 11	−18.6	157	+1.70	−21.8	157	+1.71	(4, 7)m 6m (9, 12)s 10s	(1, 2)s (4, 7)s 6s? (9, 12)s 10s	−16.1	159	+1.68
6	−23.4	172	+1.79	−26.4	171	+1.68	(5, 11)m 10m	(1, 2)s (5, 11)s? 10s	−22.4	172	+1.69
8	+8.6	142	+2.55	−0.8	*ca.* 135?[h]	+2.18	(4, 7)s, (9, 12)s	(1, 2)w[4] (4, 7)s? (9, 12)s	+6.8	144	+3.16
9, 12	−8.3	141	+1.94	−11.9	140	+2.03	(4, 7)s (5, 11)s 8s 10s	(4, 7)s (5, 11)s 8s 10s	−5.9	*h*	+2.80
10[i]	−1.8	*ca.*140?[h]	+3.36	−1.74	*ca.*135?[h]	+5.07	(5, 11)s 6m (9, 12)s	(5, 11)s 6s (9, 12)s	+3.5	145	+3.15

[a] Assignment by relative intensities and COSY correlations. [b] δ(^{1}H) related to directly bound B positions by ^{1}H-{^{11}B(selective)} experiments. [c] s = Stronger, w = weaker, m = intermediate, and ? = uncertain. [d] The observed incidence and intensity of the [^{11}B–^{11}B] correlations were essentially the same for all compounds (**1**)—(**4**) (compare ref. 1), except for the weaker correlations to ^{11}B(6) which were not observed for (**2**) under the experimental conditions at a weaker sample concentration. [e] Measured under conditions of {^{11}B(broad band)} decoupling (ref. 35). Correlations arise from $^3J(^1H-^1H)$ couplings, except where superscript *n* indicates *n*J path. [f] Signal from cluster CH unit. [g] Signal from η^5-C_5X_5 unit. [h] Values uncertain due to ^{11}B peak overlap. [i] Position antipodal to metal atom.

Table 4. Measured ^{11}B and ^{1}H n.m.r. parameters (δ/p.p.m., *J*/Hz) for *closo*-1,2-$C_2B_{10}H_{12}$ in $CDCl_3$ solution at 294—297 K

Assignment	δ(^{11}B)	Observed [^{11}B–^{11}B]-COSY correlations	δ(^{1}H)	$^1J(^{11}B-^1H)$
9, 12	−2.3	(8, 10)s (4, 5, 7, 11)s	+2.30	148
8, 10	−9.1	(9, 12)s (4, 5, 7, 11)s	+2.21	151
4, 5, 7, 11	−13.6	(9, 12)s (8, 10)s (3, 6)s	+2.13	158
3, 6	−14.7	(8, 10)s (4, 5, 7, 11)s	+2.32	158
1, 2	—	—	+3.55	—

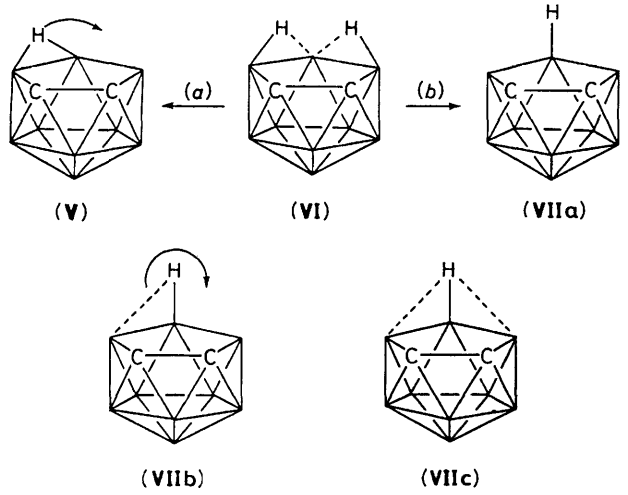

Scheme.

(h.o.m.o.s), and their symmetry-related lowest unoccupied molecular orbitals (l.u.m.o.s) that are relevant to nuclear shielding considerations, are much the same in the 3,1,2-metalladicarbaboranes as in the 1,2-dicarbadodecaborane parent itself, thereby emphasizing the isolobal and isoelectronic characteristics of BH and M(η^n-C_nMe_n).

In this regard it is also of interest to compare the metalladicarbaborane shielding patterns to those of the neutral and anionic *nido* eleven-vertex fragments 7,8-$C_2B_9H_{13}$ and [7,8-$C_2B_9H_{12}$]$^-$, particularly in view of the perspectives about metal–heteroborane bonding that arise[22,24,25,28] from a similar consideration of the shielding patterns of *nido* eleven-vertex 7,8-$C_2B_9H_{11}$,[28] 7-$SeB_{10}H_{10}$,[24] 7-$TeB_{10}H_{10}$,[22] and 7-$PhPB_{10}H_{10}$[25] units with respect to some of their complexes with platinum centres. The COSY-assigned ^{11}B and ^{1}H n.m.r. data for *nido*-7,8-$C_2B_9H_{13}$ and *nido*-7,8-$C_2B_9H_{12}^-$ are summarized in Table 5 and Figure 3. The ^{11}B assignments are in agreement with those based on labelling experiments that have been previously reported,[29–31] but the ^{1}H measurements and assignments, based on ^{1}H-{^{11}B}, and [^{1}H–^{1}H]-COSY-{^{11}B}, spectroscopy, are new.

The proton–boron-11 correlation plots for both species indicate expected behaviour, with a general parallel between the ^{11}B and ^{1}H nuclear shieldings for BH(*exo*) units for each compound, although it is interesting that the δ(^{1}H) *vs.* δ(^{11}B) slope for the neutral species is unusually flat at 1:28. A comparison between the ^{11}B shielding patterns for the two species (central part of lower diagram in Figure 3) reveals a general large increase in ^{11}B shielding upon deprotonation [δ(^{11}B)(mean) 20.9 for the anion *versus* −12.5 p.p.m. for $C_2B_9H_{13}$], probably, in view of the chemical shift changes (see next paragraph), arising from increased electronic circulations arising from a change in cluster electronic structure rather than one of increased electronic charge arising from a straightforward deprotonation. Thus, an assessment of the ^{11}B shielding changes for individual sites in $C_2B_9H_{13}$ upon deprotonation indicates generally large shielding increases of from about 10 to well over 20 p.p.m. for all sites, except for ^{11}B(3), which remains very similar, and for ^{11}B(9, 11), which *decreases* by about 15 p.p.m. These large changes and retention of symmetry seem to us at present to be incompatible with a straightforward deprotonation as in the Scheme [route (*a*)] to give a monobridged cation as in (**V**), since this would retain much of the character of the doubly bridged neutral species (**VI**). This therefore suggests an *endo*-terminal proton disposition as in (**VII**) for the anion, although the possibility cannot be ruled out that in solution there is partial bridging character, either two-site as in (**VIIb**) or triply bridging as in (**VIIc**).* Any molecular

* *Note added in proof*: Single-crystal *X*-ray diffraction analysis reveals, (see preceding paper), the symmetrical *endo* structure (**VIIa**), and extended-Hückel molecular orbital calculations suggest additional symmetrical orbital interaction between *endo*-H(10) and the B(9) and B(11) atoms [Structure (**VIIc**)].

Table 5. Measured n.m.r. parameters (δ/p.p.m., *J*/Hz) for Cs[*nido*-7,8-$C_2B_9H_{12}$][$(CD_3)_2CO$ solution] and *nido*-7,8-$C_2B_9H_{13}$(CD_2Cl_2 solution) at 294—297 K

	$Cs[C_2B_9H_{12}]$				
Assignment[a]	δ(^{11}B)	$^1J(^{11}B-^1H)$	Observed[^{11}B–^{11}B]-COSY correlations[b,c]	δ(^{1}H)[d]	Observed [^{1}H–^{1}H]-COSY correlations[b,c,e]
1	−37.8	139	(2,4)s 3s (5,6)s	+0.57	(2,4)s 3s (5,6)s (9,11)w^4 μw^4
2, 4	−22.2	148	1s 3s (5,6)m (9,11)m	+1.23	1s 3s (5,6)s? (7,8)s (9,11)s μs
3	−17.6	*ca.* 144?[f]	1s (2,4)s	+1.70	1s (2,4)s (7,8)s?
5, 6	−16.8	*f*	1s (2,4)m (9,11)m 10s	+1.25	1s (2,4)s? (9,11)s 10s μs
7, 8[g]	—	—	—	+1.70	(2,4)s 3s? (9,11)s 10s^4
9, 11	−10.9	135	2,4m (5,6)m 10s	+1.94	1w^4 (2,4)s (5,6)s (7,8)s 10m μs^2
10	−33.2	133, 52	(5,6)s (9,11)s	+0.10	(5,6)s (7,8)s^4 (9,11)m μs^2
μ-H	—	52	—	−2.89	1w^4 (2,4)s (9,11)s^2 10s^2 (5,6)s
	$C_2B_9H_{13}$				
1	−27.1	*ca.*144?[f]	(2,4)s? 3s (5,6)s	+1.65	(2,4)w 3? (5,6)m
2, 4	+4.4	163	1s? 3s (5,6)s (9,11)s	+2.92	1w (9,11)w
3	−15.8	*ca.* 176?[f]	1s (2,4)s	+1.99	1?
5,6	−4.3	151	1s (2,4)s (9,11)s 10s	+2.28	1m (7,8)m^4 (9,11)m 10s?
7,8[g]	—	—	—	+3.60	(5,6)m^4
9,11	−26.6	*ca.* 144?[f]	(2,4)s (5,6)s 10?	+1.74	(2,4)w (5,6)m μs^2
10	−16.3	*ca.* 159?[f]	(5,6)s (9,11)?	+2.15	(5,6)s? μs^2
μ-H	—	—	—	−1.59	(9,11)s^2 10s^2

[a] Assignments by relative intensities and COSY correlations (compare refs. 29 and 30). [b] Note that the strength of the *observed* correlation depends upon experimental factors such as relaxation times, dilutions *versus* number of transients accumulated, *etc.*, as well as upon the magnitude of the coupling constant. [c] s = Stronger, w = weaker, m = intermediate, and ? = uncertain. [d] δ(^{1}H) related to directly bound B positions by ^{1}H-{^{11}B(selective)} experiments. [e] Correlations arise from $^3J(^1H-^1H)$ couplings except where superscript *n* indicates ^nJ path. Measured under conditions of {^{11}B(broad-band noise)} decoupling. [f] Values uncertain due to ^{11}B peak overlap. [g] Cluster CH position, no ^{11}B resonance.

Table 6. Crystallographic data for compounds (2) and (3)*

Compound	(2)	(3)
Formula	$C_{12}H_{26}B_9Rh$	$C_{12}H_{26}B_9Ir$
M	370.54	459.86
a/pm	1 081.0(2)	1 076.3(1)
b/pm	1 278.2(1)	1 282.9(1)
c/pm	1 278.4(2)	1 292.8(2)
U/nm^3	1.7664(4)	1.7850(1)
D_x/g cm^{-3}	1.39	1.71
F(000)	752	880
μ/cm^{-1}	8.56	71.83
No. of data collected	1 854	1 831
No. observed [$I > 2\sigma(I)$]	1 756	1 712
R	0.0197	0.0286
R'	0.0204	0.0307
weighting factor *g*	0.0004	0.0003

* For both compounds: crystal system, orthorhombic; space group $P2_12_12_1$; $Z = 4$; scan width 2.0° + α-doublet splitting; scan speed 2.0—29.3° min^{-1}; $4.0 < 2\theta < 45.0°$; number of variables 215.

asymmetry, due to[9,10] bridging character as in (V), or pseudobridging tendencies as indicated by the dashed line in (VIIb), would not be seen in n.m.r. experiments because of fluxional tautomerism as indicated by the curved arrows in (V) and (VIIb). In this context the strong [^{1}H–^{1}H]-COSY correlation between this *endo*/bridging hydrogen atom and the ^{1}H(2,4) positions adjacent to CH(7, 8) may be of significance, and in a more general context it is also noteworthy that electronegative and electron-donating substituents at the 9 position in the [7,8-$C_2B_9H_{12}$]$^-$ anion may induce (V)-type behavioural tendencies at the expense of (VII)-type.[26]

The upper and lower parts of the lower diagram in Figure 3 relate the assigned ^{11}B n.m.r. chemical shifts of [$C_2B_9H_{12}$]$^-$ and $C_2B_9H_{13}$ to those of the iridadicarbaborane (3) taken as the example. It can be seen that the relationship between (3) and neutral $C_2B_9H_{13}$ is essentially random, indicating little relationship between the bonding in the $C_2B_9H_{11}$ fragments in $C_2B_9H_{13}$ and in [$(C_5Me_5)IrC_2B_9H_{11}$], thereby suggesting that a replacement of the B–H–B bridging bonds of (VI) by bonds to the metal centre, together with some donor interaction from the C(7)–C(8) bond to the metal, is not a satisfactory model for the carborane-to-metal interaction (contrast refs. 22 and 25). More shielding similarities apparently exist between the anionic [$C_2B_9H_{12}$]$^-$ fragment and the metalladicarbaborane. Thus, although there are large shifts downfield for the particular unique ^{11}B position that becomes adjacent to the metal, and also for the one that becomes antipodal to it, the shielding in the rest of the molecule is relatively unperturbed, suggesting that the nature of the $C_2B_9H_{11}$ fragment in the metalladicarbaborane is much more similar to that in the anion than to that in neutral $C_2B_9H_{13}$ (compare ref. 28).

Experimental

General.—The compounds [{Rh(η^5-C_5Me_5)Cl_2}$_2$],[32] [{Ir(η^5-C_5Me_5)Cl_2}$_2$],[32] [3,1,2-(C_5H_5)$CoC_2B_9H_{11}$],[3,4] and Cs[7,8-$C_2B_9H_{12}$][33] were prepared by the literature methods. Reactions were carried out under anaerobic conditions, although subsequent manipulations were carried out in air. Dried and degassed solvents were used throughout. Preparative thin-layer chromatography (t.l.c.) was done using 1-mm layers of silica gel G (Fluka, type GF254), made on glass plates of dimensions 200 × 200 mm^2, from water slurries followed by drying in air at 80–100 °C for 48 h. Preparative high-pressure liquid chromatography (h.p.l.c.) was carried out using a Lichrosorb Si60 (mesh 7 μm) column (Knauer) of dimensions

Table 7. Atom co-ordinates ($\times 10^4$) for compound (**2**)*

Atom	*x*	*y*	*z*	Atom	*x*	*y*	*z*
Rh(3)	4 442.7(2)	4 495.2(2)	138.3(2)	H(16c)	3 544(5)	2 019(3)	896(4)
C(11)	5 113(3)	2 954(3)	567(3)	H(17a)	4 285(5)	2 660(3)	−2 019(4)
C(12)	5 102(3)	3 011(3)	−549(3)	H(17b)	3 503(5)	2 130(3)	−930(4)
C(13)	5 942(3)	3 831(3)	−859(3)	H(17c)	4 925(5)	1 589(3)	−1 337(4)
C(14)	6 439(3)	4 274(3)	66(4)	H(18a)	5 669(5)	3 905(4)	−2 619(4)
C(15)	5 944(3)	3 745(3)	949(3)	H(18b)	7 143(5)	3 769(4)	−2 044(4)
C(16)	4 445(5)	2 180(3)	1 225(4)	H(18c)	6 349(5)	4 971(4)	−1 959(4)
C(17)	4 400(5)	2 304(3)	−1 259(4)	H(19a)	7 647(4)	5 089(4)	−706(5)
C(18)	6 245(5)	4 131(4)	−1 967(4)	H(19b)	8 186(4)	5 010(4)	594(5)
C(19)	7 386(4)	5 150(4)	107(5)	H(19c)	7 029(4)	5 924(4)	259(5)
C(110)	6 263(4)	3 917(4)	2 084(3)	H(110a)	6 807(4)	4 613(4)	1 954(3)
C(1)	3 965(3)	6 091(3)	−273(3)	H(110b)	6 869(4)	3 270(4)	2 266(3)
C(2)	2 980(3)	5 246(3)	−752(3)	H(110c)	5 636(4)	4 046(4)	2 729(3)
B(4)	4 176(4)	5 916(3)	1 062(4)	H(1)	4 679	6 312	−793
B(5)	3 246(4)	6 950(3)	535(4)	H(2)	3 125	4 978	−1 549
B(6)	2 514(4)	6 532(3)	−622(4)	H(4)	4 954	6 219	1 437
B(7)	2 423(4)	4 426(3)	195(4)	H(5)	3 720	7 753	598
B(8)	3 162(4)	4 851(3)	1 399(4)	H(6)	2 410	6 970	−1 231
B(9)	2 713(5)	6 176(3)	1 587(4)	H(7)	2 029	3 579	−164
B(10)	1 695(5)	6 563(4)	559(4)	H(8)	3 165	4 332	2 085
B(11)	1 531(4)	5 491(4)	−298(5)	H(9)	2 620	6 487	2 461
B(12)	1 641(4)	5 268(4)	1 062(5)	H(10)	894	7 137	628
H(16a)	4 346(5)	2 383(3)	2 041(4)	H(11)	782	5 258	−924
H(16b)	5 022(5)	1 494(3)	1 154(4)	H(12)	1 054	4 920	1 443

* Atomic parameters not refined.

Table 8. Atom co-ordinates ($\times 10^4$) for compound (**3**)*

Atom	*x*	*y*	*z*	Atom	*x*	*y*	*z*
Ir(3)	4 416.9(3)	4 503.9(3)	167.4(3)	H(16c)	5 067(10)	1 705(8)	1 627(10)
C(11)	5 074(9)	2 974(7)	588(8)	H(17a)	3 912(10)	1 793(9)	−781(10)
C(12)	5 134(8)	3 042(7)	−539(8)	H(17b)	5 094(10)	1 918(9)	−1 718(10)
C(13)	5 926(8)	3 849(8)	−815(8)	H(17c)	3 828(10)	2 791(9)	−1 717(10)
C(14)	6 436(8)	4 268(8)	95(9)	H(18a)	6 857(10)	4 827(10)	−1 903(9)
C(15)	5 948(9)	3 759(8)	960(8)	H(18b)	5 368(10)	4 412(10)	−2 296(9)
C(16)	4 402(10)	2 193(8)	1 231(10)	H(18c)	6 628(10)	3 534(10)	−2 324(9)
C(17)	4 446(10)	2 339(9)	−1 235(10)	H(19a)	7 581(9)	5 411(9)	−613(11)
C(18)	6 216(10)	4 180(10)	−1 913(9)	H(19b)	8 172(9)	4 899(9)	554(11)
C(19)	7 343(9)	5 154(9)	158(11)	H(19c)	6 926(9)	5 791(9)	580(11)
C(110)	6 281(11)	3 946(10)	2 083(9)	H(110a)	5 743(11)	3 432(10)	2 569(9)
C(1)	3 967(9)	6 104(7)	−243(8)	H(110b)	6 081(11)	4 746(10)	2 284(9)
C(2)	2 991(9)	5 270(7)	−726(8)	H(110c)	7 259(11)	3 794(10)	2 197(9)
B(4)	4 154(11)	5 890(9)	1 064(10)	H(1)	4 669	6 335	−791
B(5)	3 177(11)	6 902(9)	541(11)	H(2)	3 099	4 993	−1 537
B(6)	2 558(10)	6 551(10)	−613(10)	H(4)	4 958	6 200	1 438
B(7)	2 397(9)	4 389(9)	198(9)	H(5)	3 724	7 746	603
B(8)	3 038(11)	4 814(9)	1 394(10)	H(6)	2 435	6 993	−1 249
B(9)	2 610(12)	6 149(9)	1 555(10)	H(7)	2 041	3 578	−157
B(10)	1 692(11)	6 557(9)	500(11)	H(8)	3 182	4 341	2 075
B(11)	1 530(10)	5 473(9)	−307(11)	H(9)	2 597	6 477	2 440
B(12)	1 591(10)	5 274(10)	988(11)	H(10)	889	7 142	632
H(16a)	3 822(10)	1 716(8)	740(10)	H(11)	782	5 267	−937
H(16b)	3 831(10)	2 591(8)	1 793(10)	H(12)	1 048	4 923	1 426

* Atomic parameters not refined.

25 cm × 16 mm; retention times R_t are for a liquid-phase flow-rate of 10 cm^3 min^{-1}. Mass spectra were measured on an AEI (now Kratos) MS30 instrument using the solid-sample introduction probe and 70-eV (1.12×10^{-17} J) electron-impact ionization.

Nuclear Magnetic Resonance Spectroscopy.—N.m.r. spectroscopy was performed at 2.35 and 9.4 T using commercially available instrumentation. The general techniques, and the techniques of [^{11}B–^{11}B]-COSY,[34] [^{1}H–^{1}H]-COSY-{^{11}B},[35] and ^{1}H-{^{11}B}[36] spectroscopy, were essentially as described and illustrated in other recent papers describing n.m.r. work in our laboratories.[22,37–39] Chemical shifts δ are given in p.p.m. positive to high frequency (low field) of Ξ100 ($SiMe_4$) for ^{1}H (quoted ± 0.05 p.p.m.) and Ξ31.083 971 MHz (nominally $F_3B{\cdot}OEt_2$ in $CDCl_3$) for ^{11}B (quoted ± 0.5 p.p.m.), Ξ being defined as in ref. 40. The coupling constant $^1J(^{11}B–^1H)$ is quoted in Hz, and was measured from

resolution-enhanced ^{11}B n.m.r. spectra with digital resolution 8 Hz.

Single Crystal X-Ray Analysis.—All crystallographic measurements were made on a Nicolet P3/F diffractometer operating in the ω—2θ scan mode using a standard procedure described elsewhere.[41] Both sets of data were corrected for absorption empirically once their structures had been determined.[42]

The structure of rhodium complex (**2**) was determined *via* standard heavy-atom methods and refined by full-matrix least squares using the SHELX program system.[43] All non-hydrogen atoms were refined with anisotropic thermal parameters. The methyl hydrogen atoms were included in calculated positions and assigned overall isotropic parameters. However, the borane hydrogen atoms, which were located in a Fourier difference map, tended to move to unreasonable positions when refined and so they were assigned a fixed overall isotropic thermal parameter and their positional parameters not refined.

The isomorphous iridium complex (**3**) was solved using the co-ordinates of (**2**) and was refined in an identical manner. In both cases the weighting scheme $w = [\sigma^2(F_o) + g(F_o)^2]^{-1}$ was used at the end of refinement in order to obtain satisfactory agreement analyses. Crystal data, data collection and structure refinement parameters are given in Table 6 and atomic co-ordinates for compounds (**2**) and (**3**) are given in Tables 7 and 8 respectively.

Additional material available from the Cambridge Crystallographic Data Centre comprises H-atom co-ordinates, thermal parameters, and remaining bond lengths and angles.

Reaction of $[\{Rh(\eta^5\text{-}C_5Me_5)Cl_2\}_2]$ *with* $Cs[nido\text{-}7,8\text{-}C_2B_9H_{12}]$. —A solution of $[\{Rh(\eta^5\text{-}C_5Me_5)Cl_2\}_2]$ (200 mg, 324 μmol) and $Cs[7,8\text{-}C_2B_9H_{12}]$ (350 mg, 1.31 mmol) in CH_2Cl_2 (40 cm^3) was stirred at room temperature for 24 h, then heated under reflux for a further 16 h, during which time the colour of the solution paled somewhat. Filtration of the mixture over silica, with the aid of more CH_2Cl_2 (50 cm^3), gave an orange solution, which was then reduced in volume (rotary evaporator, *ca.* 20 °C, water-pump pressure) to *ca.* 10 cm^3. This solution was then subjected to h.p.l.c. separation using CH_2Cl_2–MeCN (95:5) as the liquid phase, yielding the pale orange air-stable crystalline compound (**2**), R_t 7.9—10.7 min, characterized by single-crystal *X*-ray diffraction analysis, ^{11}B and ^1H n.m.r. spectroscopy, and mass spectrometry as $[3\text{-}(\eta^5\text{-}C_5Me_5)\text{-}closo\text{-}3,1,2\text{-}RhC_2B_9H_{11}]$ (82 mg, 221 μmol; 34%) [*m/z* (maximum) 372; $^{12}C_{12}{}^1H_{26}{}^{11}B_9{}^{103}Rh$ requires 372]. A crystal suitable for *X*-ray diffraction analysis was obtained by diffusion of hexane into a solution of compound (**2**) in CH_2Cl_2.

Reaction of $[\{Ir(\eta^5\text{-}C_5Me_5)Cl_2\}_2]$ *with* $Cs[nido\text{-}7,8\text{-}C_2B_9H_{12}]$.—Samples of $[\{Ir(\eta^5\text{-}C_5Me_5)Cl_2\}_2]$ (300 mg, 380 μmol) and $Cs[7,8\text{-}C_2B_9H_{12}]$ (450 mg, 1.69 mmol) were stirred in CH_2Cl_2 (40 cm^3) for 2 h at room temperature, after which time the original orange colour changed to deep red. The mixture was stirred for a further 48 h, and filtered over silica with the aid of more CH_2Cl_2 (30 cm^3) to give a deep red filtrate A. Washing the silica with MeCN (20 cm^3) gave a second, yellow, filtrate B. Each solution was reduced in volume (rotary evaporator, *ca.* 20 °C, water-pump pressure) to *ca.* 5 cm^3. The reduced CH_2Cl_2 solution A was applied to preparative t.l.c. plates and developed using CH_2Cl_2–hexane (80:20) as the liquid phase. This resulted in the separation of a number of coloured components, of which any metallaboranes present were in unviably small yields, together with larger quantities of a yellow crystalline air-stable solid, compound (**3**), R_f 0.90, characterized by single-crystal *X*-ray diffraction analysis, ^{11}B and ^1H n.m.r. spectroscopy, and mass spectrometry as $[3\text{-}(\eta^5\text{-}C_5Me_5)\text{-}closo\text{-}3,1,2\text{-}IrC_2B_9H_{11}]$ [*m/z* (maximum) 462; $^{12}C_{12}{}^1H_{26}{}^{11}B_9{}^{193}Ir$ requires 462]. Addition of CH_2Cl_2 (20 cm^3) to the reduced MeCN solution B resulted in the precipitation of white solid (identified by n.m.r. spectroscopy as a salt of the starting $[C_2B_9H_{12}]^-$ anion), and in the darkening of the solution to orange. The filtered solution was reduced to dryness (rotary evaporator *ca.* 20 °C; water-pump pressure) and dissolved in CH_2Cl_2–MeCN (90:10). The resulting solution was subjected to h.p.l.c. separation using CH_2Cl_2–MeCN (98:2) as mobile liquid phase, yielding a further sample of (**3**), R_t 9.1 min. The combined yield of (**3**) was 334 mg, 726 μmol, 96%; crystals suitable for the *X*-ray diffraction experiments were grown from a CH_2Cl_2 solution of the compound overlayered by hexane.

Acknowledgements

We thank the S.E.R.C. for support and for a maintenance grant (to K. N.), the Royal Society and the British Council for travel funds, and Mr D. Singh for the mass spectrometric results.

References

1 M. Bown, J. Plešek, K. Baše, B. Štíbr, X. L. R. Fontaine, N. N. Greenwood, and J. D. Kennedy, *Magn. Reson. Chem.*, 1989, **27**, 947.
2 M. Bown, X. L. R. Fontaine, N. N. Greenwood, J. D. Kennedy, J. Plešek, B. Štíbr, and M. Thornton-Pett, *Acta Crystallogr. Sect. C*, 1989, in the press.
3 M. F. Hawthorne, D. C. Young, T. D. Andrews, D. W. Howe, R. L. Pilling, A. D. Pitts, M. Reintjes, L. F. Warren, and P. A. Wegner, *J. Am. Chem. Soc.*, 1968, **90**, 879.
4 J. Plešek, B. Štíbr, and S. Heřmánek, *Synth. Inorg. Met. Org. Chem.*, 1973, **3**, 291; J. Plešek, S. Heřmánek, and B. Štíbr, *Inorg. Synth.*, 1982, **22**, 235.
5 M. Bown, T. Jelínek, B. Štíbr, S. Heřmánek, X. L. R. Fontaine, N. N. Greenwood, J. D. Kennedy, and M. Thornton-Pett, *J. Chem. Soc., Chem. Commun.*, 1988, 974.
6 M. Bown, X. L. R. Fontaine, N. N. Greenwood, J. D. Kennedy, and M. Thornton-Pett, *J. Chem. Soc., Chem. Commun.*, 1987, 1650.
7 See, for example, X. L. R. Fontaine, N. N. Greenwood, J. D. Kennedy, P. MacKinnon, and M. Thornton-Pett, *J. Chem. Soc., Dalton Trans.*, 1988, 2809 and refs. therein.
8 Faridoon, M. McGrath, T. R. Spalding, X. L. R. Fontaine, J. D. Kennedy, and M. Thornton-Pett, *J. Chem. Soc., Dalton Trans.*, 1989, in the press (Paper 9/03254A).
9 M. Bown, X. L. R. Fontaine, H. Fowkes, N. N. Greenwood, J. D. Kennedy, P. MacKinnon, and K. Nestor, *J. Chem. Soc., Dalton Trans.*, 1988, 2597.
10 K. Nestor, X. L. R. Fontaine, N. N. Greenwood, J. D. Kennedy, and M. Thornton-Pett, *J. Chem. Soc., Chem. Commun.*, 1989, 455.
11 K. Nestor, X. L. R. Fontaine, N. N. Greenwood, J. D. Kennedy, and M. Thornton-Pett, *J. Chem. Soc., Dalton Trans.*, 1989, 1465.
12 K. Nestor, X. L. R. Fontaine, N. N. Greenwood, J. D. Kennedy, and M. Thornton-Pett, *J. Chem. Soc., Dalton Trans.*, unpublished work.
13 K. Nestor, B. Štíbr, X. L. R. Fontaine, N. N. Greenwood, K. Baše, J. D. Kennedy, and M. Thornton-Pett, unpublished work.
14 K. Baše, M. Bown, B. Štíbr, X. L. R. Fontaine, N. N. Greenwood, J. D. Kennedy, and M. Thornton-Pett, *J. Chem. Soc., Chem. Commun.*, 1988, 1240.
15 M. Bown, X. L. R. Fontaine, N. N. Greenwood, J. D. Kennedy, and M. Thornton-Pett, *Organometallics*, 1987, 2254.
16 D. M. P. Mingos, M. I. Forsyth, and A. J. Welch, *J. Chem. Soc., Chem. Commun.*, 1977, 605; *J. Chem. Soc., Dalton Trans.*, 1978, 1363.
17 H. M. Colquhoun, T. J. Greenhough, and M. G. H. Wallbridge, *J. Chem. Soc., Dalton Trans.*, 1979, 619.
18 M. Bown, X. L. R. Fontaine, N. N. Greenwood, J. D. Kennedy, and M. Thornton-Pett, *J. Chem. Soc., Dalton Trans.*, submitted for publication.
19 K. Nestor, X. L. R. Fontaine, N. N. Greenwood, J. D. Kennedy, J. Plešek, B. Štíbr, and M. Thornton-Pett, *Inorg. Chem.*, 1989, **28**, 2219.
20 R. E. Williams, *Inorg. Chem.*, 1971, **10**, 210; *Adv. Inorg. Chem. Radiochem.*, 1976, **18**, 67.

21 K. Wade, *Chem. Commun.*, 1971, 792; *Adv. Inorg. Chem. Radiochem.*, 1976, **18**, 1.
22 J. Ferguson, J. D. Kennedy, X. L. R. Fontaine, Faridoon, and T. R. Spalding, *J. Chem. Soc., Dalton Trans.*, 1988, 2555.
23 Faridoon, O. Ni Dhubhghaill, T. R. Spalding, G. Ferguson, B. Kaitner, X. L. R. Fontaine, J. D. Kennedy, and D. Reed, *J. Chem. Soc., Dalton Trans.*, 1988, 2739.
24 Faridoon, O. Ni Dhubhghaill, T. R. Spalding, G. Ferguson, X. L. R. Fontaine, and J. D. Kennedy, *J. Chem. Soc., Dalton Trans.*, 1989, 1657.
25 S. R. Bunkhall, X. L. R. Fontaine, N. N. Greenwood, J. D. Kennedy, and M. Thornton-Pett, *J. Chem. Soc., Dalton Trans.*, 1990, 151.
26 See, for example, S. Heřmánek, T. Jelínek, J. Plešek, B. Štíbr, J. Fusek, and F. Mareš, in 'Boron Chemistry (IMEBORON VI),' ed. S. Hařmánek, World Scientific, Singapore, 1987, p. 26, and refs therein.
27 M. Bown, X. L. R. Fontaine, N. N. Greenwood, and J. D. Kennedy, *J. Organomet. Chem.*, 1987, **325**, 233.
28 X. L. R. Fontaine and J. D. Kennedy, University of Leeds, unpublished work.
29 A. R. Siedle, G. M. Bodner, and L. J. Todd, *J. Organomet. Chem.*, 1971, **33**, 137.
30 D. V. Howe, C. J. Jones, R. J. Wiersema, and M. F. Hawthorne, *Inorg. Chem.*, 1971, **10**, 2156.
31 S. Heřmánek, unpublished work.
32 J. W. Kong, K. Mosely, and P. M. Maitlis, *J. Am. Chem. Soc.*, 1969, **91**, 5970.
33 J. Plešek, S. Heřmánek, and B. Štíbr, *Inorg. Synth.*, 1982, **22**, 231.
34 T. L. Venable, W. C. Hutton, and R. N. Grimes, *J. Am. Chem. Soc.*, 1984, **106**, 29.
35 X. L. R. Fontaine and J. D. Kennedy, *J. Chem. Soc., Chem. Commun.*, 1986, 779.
36 J. D. Kennedy and N. N. Greenwood, *Inorg. Chim. Acta*, 1980, **38**, 529.
37 X. L. R. Fontaine and J. D. Kennedy, *J. Chem. Soc., Dalton Trans.*, 1987, 1573.
38 M. Bown, X. L. R. Fontaine, and J. D. Kennedy, *J. Chem. Soc., Dalton Trans.*, 1988, 1467.
39 M. A. Beckett, M. Bown, X. L. R. Fontaine, N. N. Greenwood, J. D. Kennedy, and M. Thornton-Pett, *J. Chem. Soc., Dalton Trans.*, 1988, 1969.
40 W. McFarlane, *Proc. R. Soc. London, Ser. A*, 1968, **306**, 185.
41 A. Modinos and P. Woodward, *J. Chem. Soc., Dalton Trans.*, 1974, 2065.
42 N. Walker and D. Stuart, *Acta Crystallogr., Sect. A*, 1983, **39**, 158.
43 G. M. Sheldrick, SHELX 76, Program System for *X*-Ray Structure Determination, University of Cambridge, 1976.

Received 16*th June* 1989; *Paper* 9/02537E